ADVANCES IN ATMOSPHERIC SCIENCES, VOL. 31, JULY 2014, 888–900

Effects of Meridional Sea Surface Temperature Changes on Stratospheric Temperature and Circulation

HU Dingzhu[1], TIAN Wenshou*[1], XIE Fei[2], SHU Jianchuan[3], and Sandip DHOMSE[4]

[1]*College of Atmospheric Sciences, Lanzhou University, Lanzhou* 730000
[2]*Institute of Atmospheric Physics, Chinese Academy of Sciences, Beijing* 100029
[3]*Institute of Plateau Meteorology, China Meteorological Administration, Chengdu* 610000
[4]*Institute for Climate and Atmospheric Science, School of Earth and Environment, University of Leeds, UK*

(Received 23 July 2013; revised 10 October 2013; accepted 11 November 2013)

ABSTRACT

Using a state-of-the-art chemistry-climate model, we analyzed the atmospheric responses to increases in sea surface temperature (SST). The results showed that increases in SST and the SST meridional gradient could intensify the subtropical westerly jets and significantly weaken the northern polar vortex. In the model runs, global uniform SST increases produced a more significant impact on the southern stratosphere than the northern stratosphere, while SST gradient increases produced a more significant impact on the northern stratosphere. The asymmetric responses of the northern and southern polar stratosphere to SST meridional gradient changes were found to be mainly due to different wave properties and transmissions in the northern and southern atmosphere. Although SST increases may give rise to stronger waves, the results showed that the effect of SST increases on the vertical propagation of tropospheric waves into the stratosphere will vary with height and latitude and be sensitive to SST meridional gradient changes. Both uniform and non-uniform SST increases accelerated the large-scale Brewer–Dobson circulation (BDC), but the gradient increases of SST between 60°S and 60°N resulted in younger mean age-of-air in the stratosphere and a larger increase in tropical upwelling, with a much higher tropopause than from a global uniform 1.0 K SST increase.

Key words: numerical simulation, stratospheric temperature, sea surface temperature, Brewer–Dobson circulation

Citation: Hu, D. Z., W. S. Tian, F. Xie, J. C. Shu, and S. Dhomse, 2014: Effects of meridional sea surface temperature changes on stratospheric temperature and circulation. *Adv. Atmos. Sci.*, **31**(4), 888–900, doi: 10.1007/s00376-013-3152-6.

1. Introduction

It is widely accepted that the Brewer–Dobson Circulation (BDC) will strengthen under the future climate due to increasing greenhouse gases (GHGs) and associated SST changes (e.g., Garcia and Randel, 2008, Xie et al., 2008; Shu et al., 2011). Subsequently, some studies have argued that BDC is mainly affected by SST changes and that radiative effects of GHGs are less important than the SST changes in modulating tropical upwelling (Xie et al., 2008). Deckert and Dameris (2008) suggested that warmer tropical SSTs will strengthen the lower-stratospheric BDC in the tropics in the summer hemisphere via enhancing deep-convective generation of upward propagating quasi-stationary eddies. Some other studies have shown that SST changes can modulate BDC by changing propagation properties of synoptic and planetary-scale waves both in the troposphere and stratosphere (e.g., Butchart et al., 2006, 2010; Shepherd and McLandress, 2011).

Although some of the above-mentioned studies have revealed the importance of SST changes in modulating stratospheric circulation, the underlying mechanisms are still under debate. Global SST changes are not uniform, and any local SST changes are likely to cause changes in zonal and meridional SST gradients. Chiang et al. (2002) found that the local meridional SST gradient is one of the dominant factors in controlling boreal spring Atlantic Intertropical Convergence Zone variability. Hoerling et al. (2001) demonstrated that the progressive warming of the equatorial oceans is associated with climate changes over the North Atlantic, and warmer tropical SSTs force a positive North Atlantic Oscillation phase; and this was further confirmed by Magnusdottir et al. (2004). Brierley and Fedorov (2010) revealed that the impacts over North America of changes in the meridional SST gradient are somewhat stronger than those from zonal SST variations. Some earlier studies (e.g., Rind et al., 1990; Olsen et al., 2007) provided evidence that an enhanced SST meridional gradient results in a greater meridional temperature gradient in the subtropical troposphere. The upper tropo-

* Corresponding author: TIAN Wenshou
Email: wstian@lzu.edu.cn

spheric zonal winds then increase following the thermal wind relationship, and hence there are more vertically-propagating waves being refracted poleward.

Obviously, SST changes have important implications on regional and global circulation. However, most climate model simulations are performed by prescribing globally uniform SST increases (e.g., Shu et al., 2011), and the impacts of SST gradient changes on stratospheric circulation and temperatures are rarely discussed. Both modeling and observational studies have shown that the SST changes associated with ENSO events have significant effects not only on tropospheric circulation (e.g., Seager et al., 2003; Feng et al., 2013) but also on stratospheric circulation (e.g., Manzini et al., 2006; Xie et al., 2011, 2012). The BDC, for instance, is strengthened during warm phases of ENSO events via enhancement of the vertical propagation of waves (e.g., Sassi et al., 2004; Calvo et al., 2010). However, ENSO evolves both local SST changes and SST gradient changes, and the relative importance of SST changes and SST gradient changes in modulating stratospheric temperature and circulation still remains unclear.

This paper focuses on diagnosing the potential effects of SST meridional gradient changes on stratospheric temperature and circulation based on a series of time-slice simulations aimed at obtaining equilibrium solutions to specified or prescribed forcing of the atmosphere using a state-of-the-art chemistry–climate model (CCM). The remainder of the text is organized as follows. Section 2 provides a brief description of the model and numerical experiments. Section 3 presents the temperature and circulation responses to different prescribed SST gradient changes, followed by an analysis in section 4 of the changes in mean age-of-air, cross-tropopause mass transport associated with the BDC, and tropical tropopause. A summary and conclusions are provided in section 5.

2. Model and numerical Experiments

The numerical tool used in this study was the well-established general circulation model, the Whole Atmosphere Community Climate Model, version 3 (WACCM3). The model has 66 vertical levels from the ground to 5.96×10^{-6} hPa, and shows good performance in simulating stratospheric processes (cf. Eyring et al., 2005; 2006). Further details regarding the model can be found in Garcia et al. (2007).

The four time-slice simulations discussed in this paper were performed at a $4^\circ(\text{lat}) \times 5^\circ(\text{lon})$ horizontal resolution with interactive chemistry. The control run (E1) used annually repeating observed monthly mean climatological SSTs from 1995 to 2000, as compiled by the Hadley Centre, UK (http://hadobs.metoffice.com/). A schematic representation of the SST configurations in runs E2, E3, and E4 is shown in Fig. 1. In run E2, the global SSTs were uniformly increased by 1.0 K relative to those in the control run, E1. In run E3, SSTs were increased linearly from the tropics (1 K) to either pole (0 K). In run E4, SST changes were similar to E3, but at a steeper rate, i.e., the temperature of 1 K was included only between the tropics and 60° in both hemispheres. The magnitudes of the SST gradient changes were a function of latitude only; sea temperature and sea-ice feedbacks were not considered in the model simulations. For the purpose of diagnosing the effects of SST changes in a more straightforward manner, and to avoid signals due to GHG changes, all the runs used the same GHG loadings, which were adopted from the Intergovernmental Panel on Climate Change (IPCC) AR4 A1B scenario (IPCC, 2007) averaged over the period 1995–2000. In all the simulations, one passive tracer was released with an arbitrary value of 1 kg kg^{-1} in the source region during the first month of the integrations, and then set to zero thereafter (hereafter, this tracer is referred to as the age-of-air tracer). The age-of-air tracer was released at the model's surface in the latitude range of 90°S to 90°N. All experiments were run for 44 years, with the first four years used as the model spin-up, and the remaining 40 years of model outputs used for analysis.

3. Temperature and circulation responses to SST gradient changes

Figure 2 shows the responses of zonal and annual mean temperature to different SST changes. The light (dark) shaded areas denote regions where the differences between sensitivity runs and the control run are statistically significant at the 95% (99%) confidence level according to the Student's *t*-test. It is apparent that temperature responses to the different SST changes had large spatial variations with different magnitudes, although the spatial patterns of the temperature response were overall similar in runs E2, E3 and E4. A global uniform 1 K SST increase (E2) caused significant warming in the troposphere. A maximum warming of about 1.5 K in the tropical upper troposphere (UT) and a maximum cooling of about 0.9 K in the tropical lower stratosphere (LS) were clearly seen (Fig. 2a). When SSTs were increased non-uniformly between the most northern and southern oceans, tropospheric warming and tropical lower stratospheric cool-

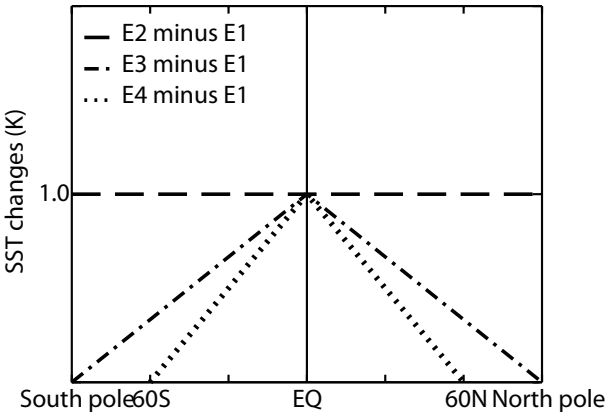

Fig. 1. A schematic representation of the SST configurations in the three simulations (see the text for more details).

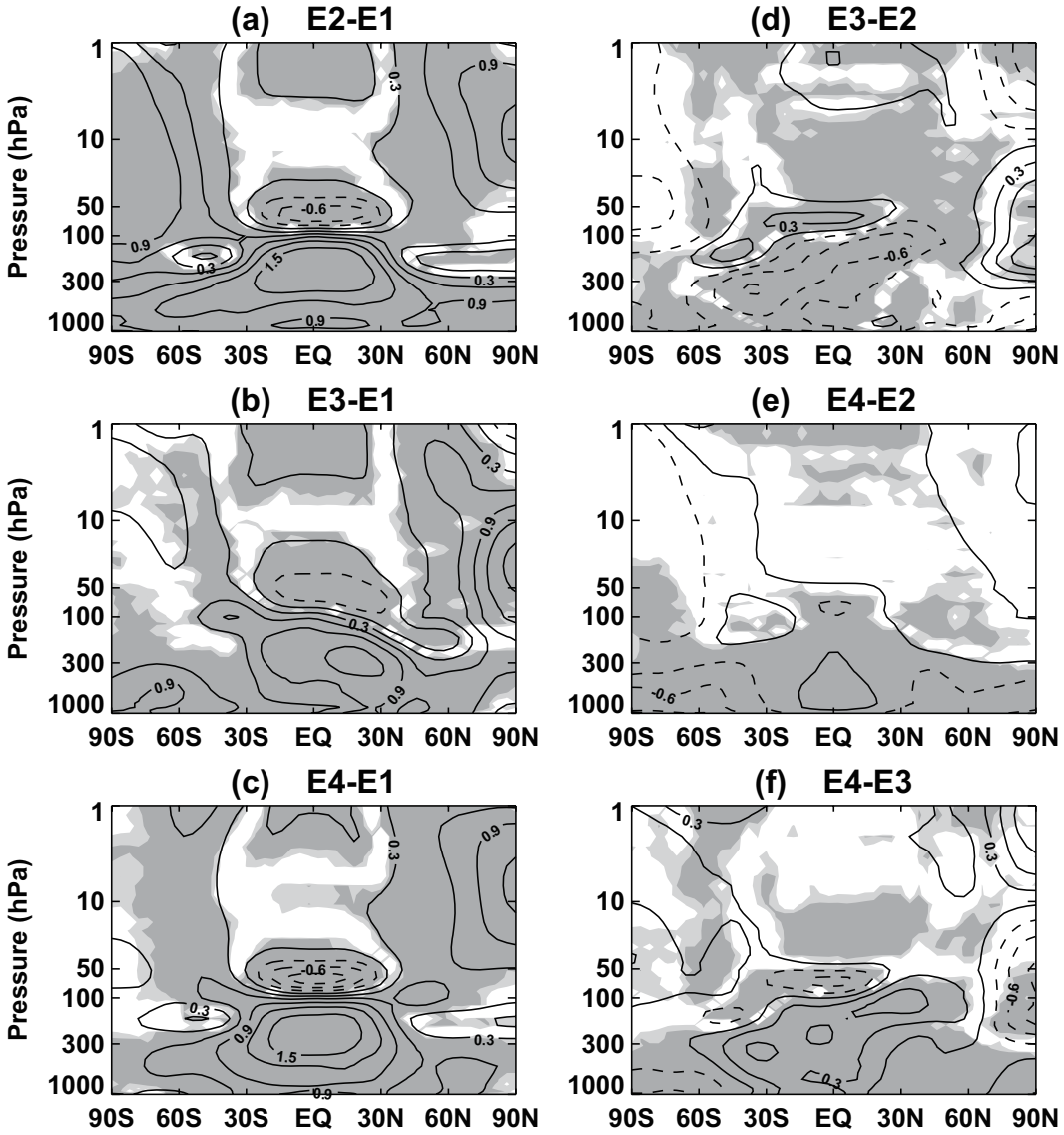

Fig. 2. The annual and zonal mean temperature differences between runs (a) E2 and E1, (b) E3 and E1, (c) E4 and E1, (d) E3 and E2, (e) E4 and E2, and (f) E4 and E3. The contour interval for temperature differences is 0.3 K. Regions where differences are statistically significant at the 95% (99%) level are shaded light (dark) grey. Solid and dashed lines represent positive and negative contours, respectively.

ing were also evident (Fig. 2b), but the temperature changes were smaller than those caused by a global uniform 1.0 K SST increase. The temperature changes at lower latitudes in E4 (Fig. 2c), in which SSTs were increased non-uniformly between 60°S and 60°N, were larger than the corresponding temperature changes in E3, showing that a larger SST meridional gradient tends to give rise to stronger temperature responses in the troposphere and LS at lower latitudes. The temperature responses in the extratropics caused by a uniform 1.0 K SST increase were in accordance with those in Shu et al. (2011). However, without interactive chemical processes in their model, Shu et al. (2011) reported a cooling in the tropical middle-upper stratosphere when global SSTs were increased uniformly. In our simulations, interactive chemical processes were switched on, and a uniform 1 K SST increase in the model generated a slight warming in the tropical middle stratosphere (Fig. 2a). Also, the global mean SST increases in runs E2, E3 and E4 were 1.0 K, 0.52 K, and 0.36 K, respectively, and it is understandable that the temperature responses in the troposphere in E2 were overall larger than those in E3 and E4.

A comparison of the temperature responses in runs E2 and E3 indicated that the warming in the troposphere at lower latitudes and the cooling in the tropical LS in E3 were smaller than those in E2, while the warming of the northern high latitude LS in E3 was larger than that in E2 (Fig. 2d). This suggests that SST gradient changes have a larger impact on the northern high latitude stratosphere than global uniform SST changes. The temperature differences between runs E4 and E3 (Fig. 2f) were almost opposite to those between runs E3 and E2 (Fig. 2d). Figure 2f indicates that the larger meridional SST gradient in E4 gave rise to a warmer tropical and

extratropical troposphere compared to E3. The temperature differences between runs E4 and E2 were relatively small (Fig. 2e), but a slight statistically significant warming in the tropical troposphere in run E4 could still be seen, further confirming that a larger meridional SST gradient can cause a warmer troposphere at lower latitudes. Taking the global mean temperature between1000–100 hPa for comparison, the warming was larger in E2 (241.1 K) than in E4 (240.9 K), in accordance with the fact that the global mean SST increase in E2 was larger than in E4. In the LS, the percentage differences of ozone between runs E4 and E1 (Fig. 3d) was larger than that between runs E2 and E1 (Fig. 3f), which was mainly due to the stronger tropical upwelling in E4, as will be discussed in more details in section 4. The more significant cooling in the LS in E4 was likely caused by the larger ozone decreases in the tropical LS. Also noticeable was that the temperature responses to SST gradient changes in E3 and E4 were more pronounced in the northern polar stratosphere than in the southern polar stratosphere. However, the temperature responses to a global uniform 1.0 K SST increase in E2 were more pronounced in the southern polar stratosphere (Fig. 2a).

Stratospheric temperatures are not only affected by SST-driven dynamical changes, but also influenced radiatively by ozone and other GHG changes (e.g., Santer et al., 2003; Solomon et al., 2007). Figure 2 reveals that the temperature in the tropical LS decreased in runs E2, E3 and E4. This decrease of the tropical LS temperature was closely related to the enhanced tropical upwelling (e.g., Bekki et al., 2013) and was amplified by the ozone changes caused by SST increases. Figure 3 shows the stratospheric ozone differences and percentage differences between runs E2 and E1, E3 and E1, and E4 and E1. The ozone in the tropical LS decreased while ozone in the tropical middle stratosphere increased in

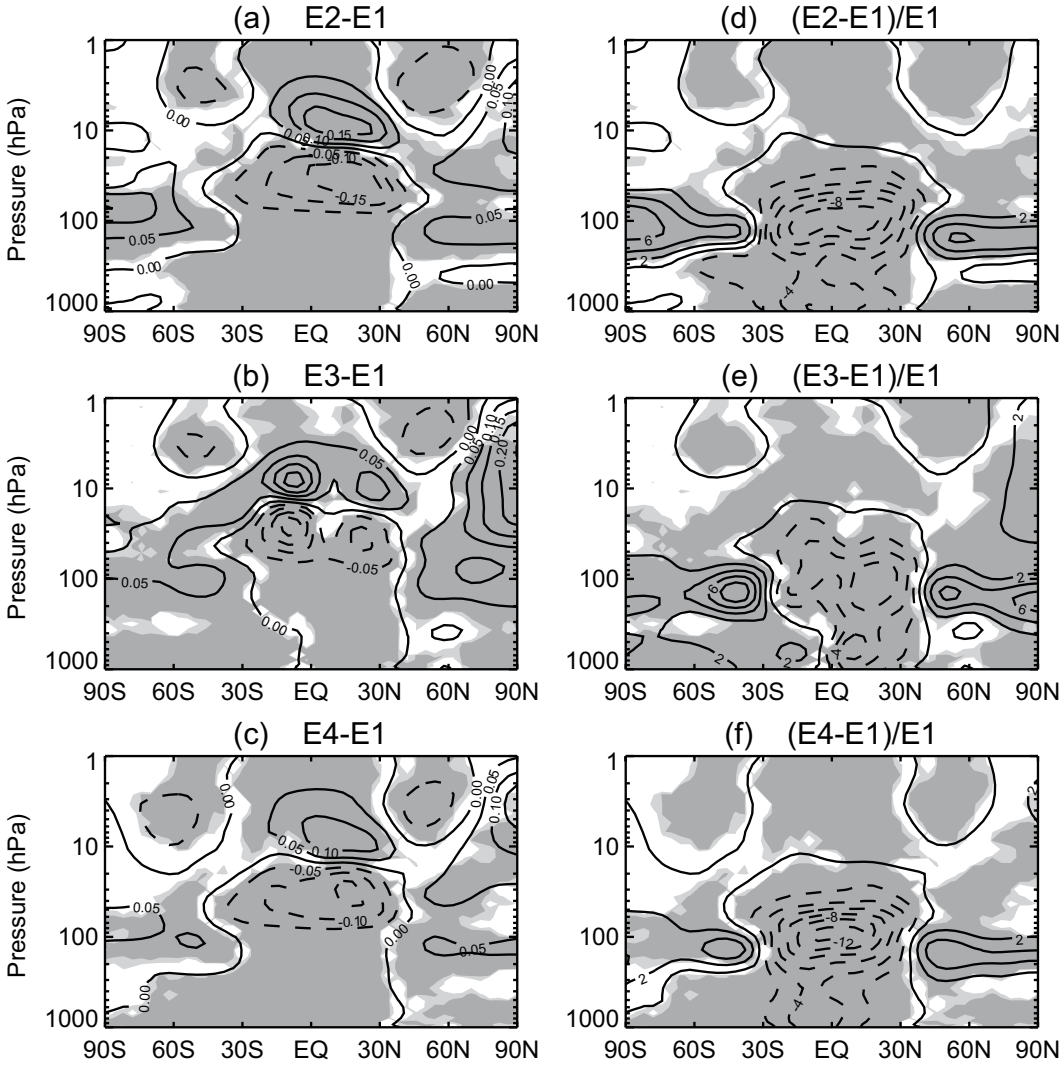

Fig. 3. Latitude–pressure cross sections of annual and zonal mean ozone (a–c) differences and (d–f) percentage differences between runs (a, d) E2 and E1, (b, e) E3 and E1, and (c, f) E4 and E1. The contour intervals for ozone differences and percentage differences are 0.05 ppmm and 2%, respectively. Solid and dashed lines represent positive and negative contours, respectively. The regions where differences are statistically significant at the 95% (99%) level are shaded light (dark) grey.

runs E2, E3 and E4, relative to that in the control run, E1. The results of our simulations with chemistry coupling suggest that ozone increases in the tropical middle stratosphere will cause a slight warming in this region (Fig. 2). However, this warming is offset by the thermodynamic effects of SST increases, which tend to cause a slight cooling in this region, as reported by Shu et al. (2011).

Figure 3 also indicates that the SST increases in runs E2, E3, and E4 caused slight ozone increases in the Arctic stratosphere and Antarctic LS. Shu et al. (2011) showed that, even without chemistry coupling in the model, the polar stratosphere is warmed when SSTs increase. Temperature increases in the polar stratosphere tend to suppress the formation of polar stratospheric clouds and cause ozone increases in the Arctic stratosphere and Antarctic LS via slowing down heterogeneous ozone destruction processes, while ozone increases will further increase temperatures in the polar stratosphere. Therefore, the warming of the Arctic stratosphere and Antarctic polar stratosphere, as exhibited in Fig. 2, is not only caused by dynamic processes, but also related to interactive chemical processes that change ozone concentrations, and in turn cause temperature changes via radiative feedback.

Figure 4 shows the responses of zonal and annual mean zonal wind to different SST changes, with the corresponding changes of Eliassen–Palm (EP) flux vectors superimposed. The different SST changes also generated different circulation responses, although the subtropical westerly jets were intensified in all three runs (Figs. 4a–c). Changes in jet

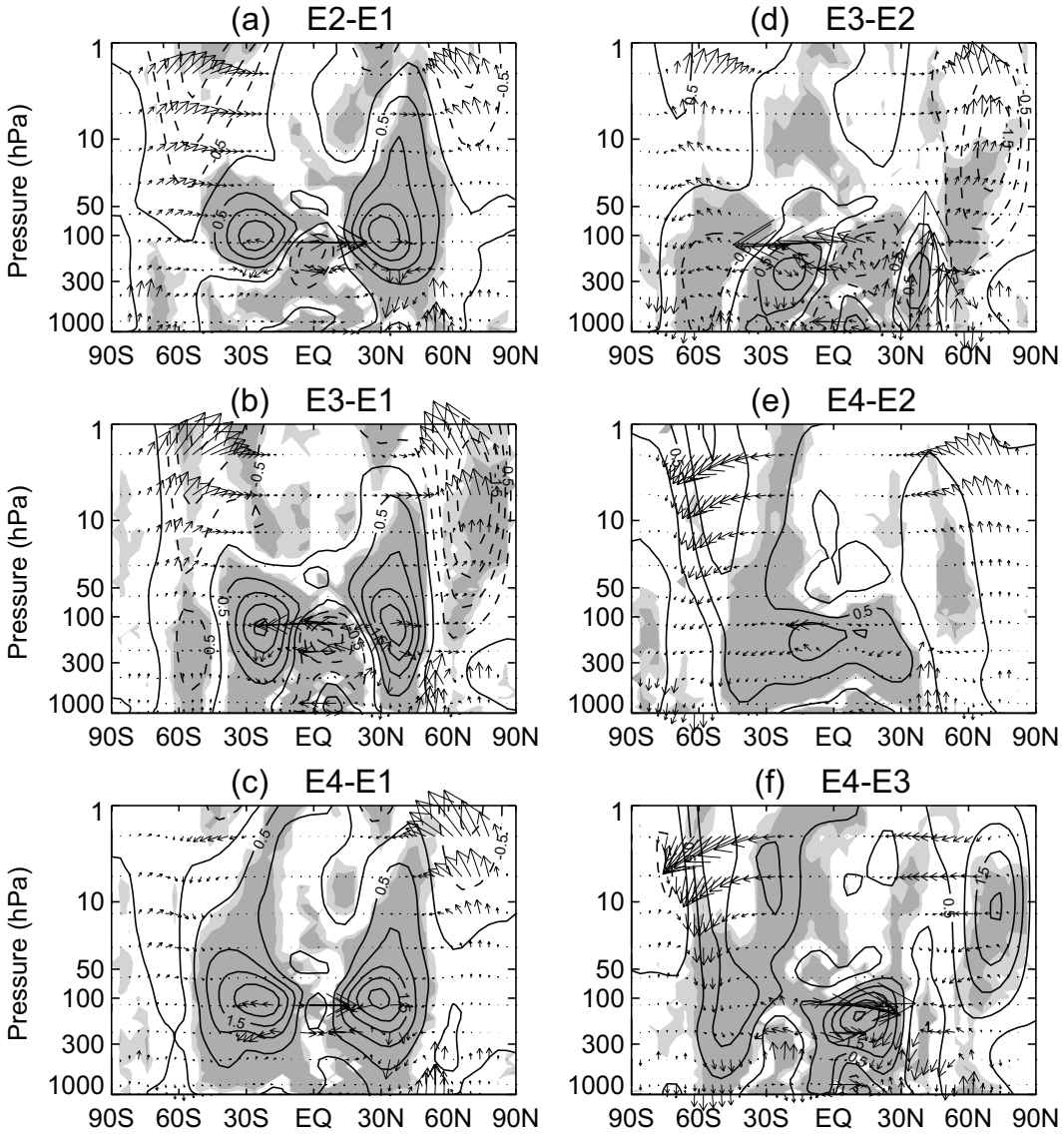

Fig. 4. The differences of annual mean zonal wind (contour lines) and differential EP flux vectors (arrows) between runs (a) E2 and E1, (b) E3 and E1, (c) E4 and E1, (d) E3 and E2, (e) E4 and E2, and (f) E4 and E3. The contour interval for zonal wind anomalies is 0.5 m s^{-1}. The unit horizontal vector is 10^9 kg s^{-2} and the unit vertical vector is 0.5×10^7 kg s^{-2} in (a)–(c), and 0.25×10^7 kg s^{-2} in (d)–(f). The regions where differences are statistically significant at the 95% (99%) level are shaded light (dark) grey. Solid and dashed lines represent positive and negative contours, respectively.

strengths are largely due to mid-latitude temperature meridional gradient changes caused by SST changes. Previous studies have also shown that SST increases tend to enhance the mid-latitude westerlies in winter and summer (Kodama et al., 2007). Figs. 4a–c shows that the zonal wind variations at lower-middle latitudes were not only related to the magnitude of SST changes, but also depend on SST meridional gradient changes. In accordance with the temperature responses in Figs. 2a–c, the SST meridional gradient changes in E3 and E4 had a greater impact on zonal circulations than the global uniform SST change in E2, particularly in the upper troposphere and lower stratosphere (UTLS) at lower-mid latitudes (Figs. 4a–b). The differences in zonal wind between runs E2, E3 and E4 showed that the enhancement of subtropical jets in E4, in which the meridional SST gradient was the steepest, was the most pronounced (Figs. 4d–f).

It is interesting that zonal winds in the northern polar stratosphere were weakest in E3, i.e., the response to SST gradient changes spanning the entire globe was stronger than the response to a uniform SST increase. However, even with a stronger SST gradient between 60° and the equator in E4, the responses of northern polar stratospheric temperatures and zonal winds were smaller than in E3. This might have been partly due to the lack of SST changes poleward of 60°N in E4. Overall, the SST increases in E2, E3 and E4 warmed the northern polar stratosphere (Fig. 2) and weakened the westerlies in the northern high-latitude upper stratosphere (Fig. 4). There were no statistically significant differences in zonal wind in the southern polar stratosphere between all the three runs and the control run. However, a weakening of the zonal winds in the southern mid-latitude upper stratosphere was evident in runs E2 and E3.

Figure 5 further shows normalized annual mean meridional temperature gradient changes (normalized by the meridional temperature gradient in E1) over the latitude bands 15°–45°N and 15°–45°S in runs E2, E3 and E4 relative to the control run, E1. The gradients were obtained from the temperature differences of 15°S minus 45°S and 15°N minus 45°N. The SST increases with meridional gradient changes resulted in greater meridional temperature gradients in the subtropical troposphere, and the larger SST meridional temperature gradient gave rise to larger meridional temperature gradients in the subtropical troposphere. Changes in the meridional temperature gradients in the subtropical troposphere will alter the structure of zonal wind through the thermal wind relationship and modify the propagation of planetary waves (e.g., Olsen et al., 2007; Shepherd and McLandress, 2011).

The differential EP flux vectors shown in Figs. 4a–c indicate that both uniform and non-uniform SST increases tend to enhance the upward propagation of planetary waves in the stratosphere at mid-high latitudes, and waves in the subtropical UTLS region tend to be refracted poleward due to the intensified subtropical westerly jets. The enhanced wave propagation from the troposphere into the stratosphere towards northern mid-high latitudes results in a warmer Arctic stratosphere, as is evident in Fig. 2. A similar result was also obtained in previous studies (e.g., Chen et al., 2002; Chen and Huang, 2002), in which it was shown that anomalous upward propagation of planetary waves into the polar waveguide across the tropopause and its interaction with mean flows leads to polar stratosphere warming in boreal winter. It is interesting that the temperature and zonal wind responses in the southern high-latitude stratosphere were small and statistically insignificant in runs E3 and E4. A careful examination of Figs. 4b and 4c reveals that the enhancement of upward propagation of waves in the lower troposphere in the southern mid-latitudes was less pronounced than that in the northern mid-latitudes. This may be one reason why the southern

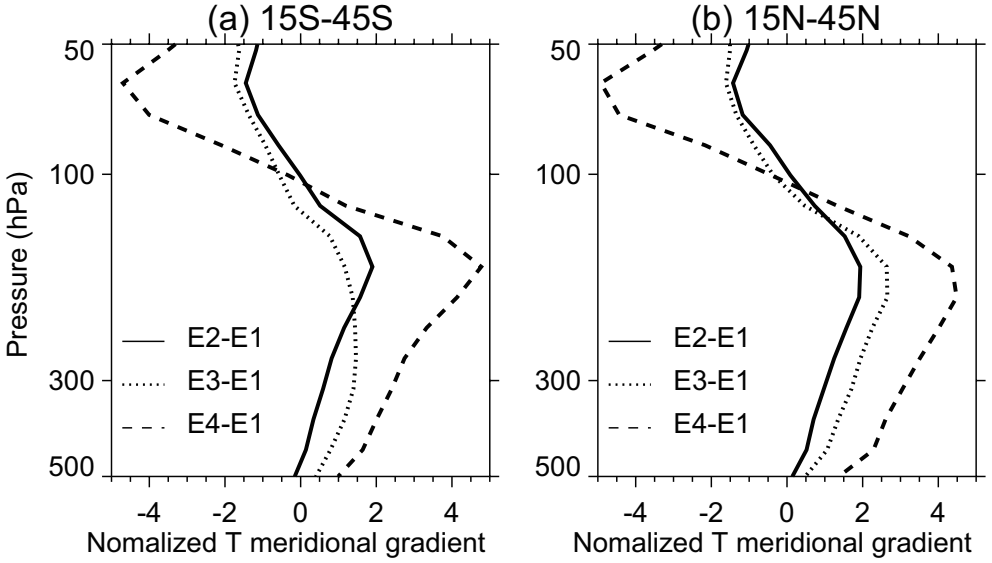

Fig. 5. The normalized annual mean meridional temperature gradient changes (normalized by the meridional temperature gradient in run E1) over the latitude band (a) 15°–45°N and (b) 15°–45°S in runs E2 (solid lines), E3 (dotted lines) and E4 (dashed lines), relative to run E1.

polar stratosphere was not significantly disturbed by the SST increases. Also noticeable was that there was enhancement of the upward propagation of waves in the southern mid-high-latitude upper stratosphere in runs E2 and E3, but this enhancement was rather weak in E4 in which SSTs were non-uniformly increased between 60°S and 60°N (Fig. 4c).

The stratospheric temperature and zonal wind responses in the tropics showed no significant seasonal variations. However, their seasonal variations were large in the high-latitude stratosphere, with the largest responses in the winter hemisphere and the smallest responses in the summer hemisphere (not shown). The stratospheric warming and zonal wind changes caused by the SST increases were larger in boreal winter than in austral winter. Figure 6 shows the responses of zonal mean temperature and zonal wind in the Northern Hemisphere (NH) averaged over December, January and February (DJF), and in the Southern Hemisphere (SH) averaged over June, July and August (JJA), to different SST changes in E2 to E4. The temperature and zonal wind responses to different SST changes in the northern winter hemisphere were similar to those of annual mean. In boreal winter, the northern polar vortex was the weakest in E3, while the temperature and zonal wind differences in the northern polar stratosphere between runs E2 and E4 were rather small. In austral winter, the polar vortex was much warmer in runs E2 and E3 than that in run E4, partly due to the lack of SST changes in polar regions in run E4. The zonal wind changes in runs E2, E3 and E4 showed no significant weakening of

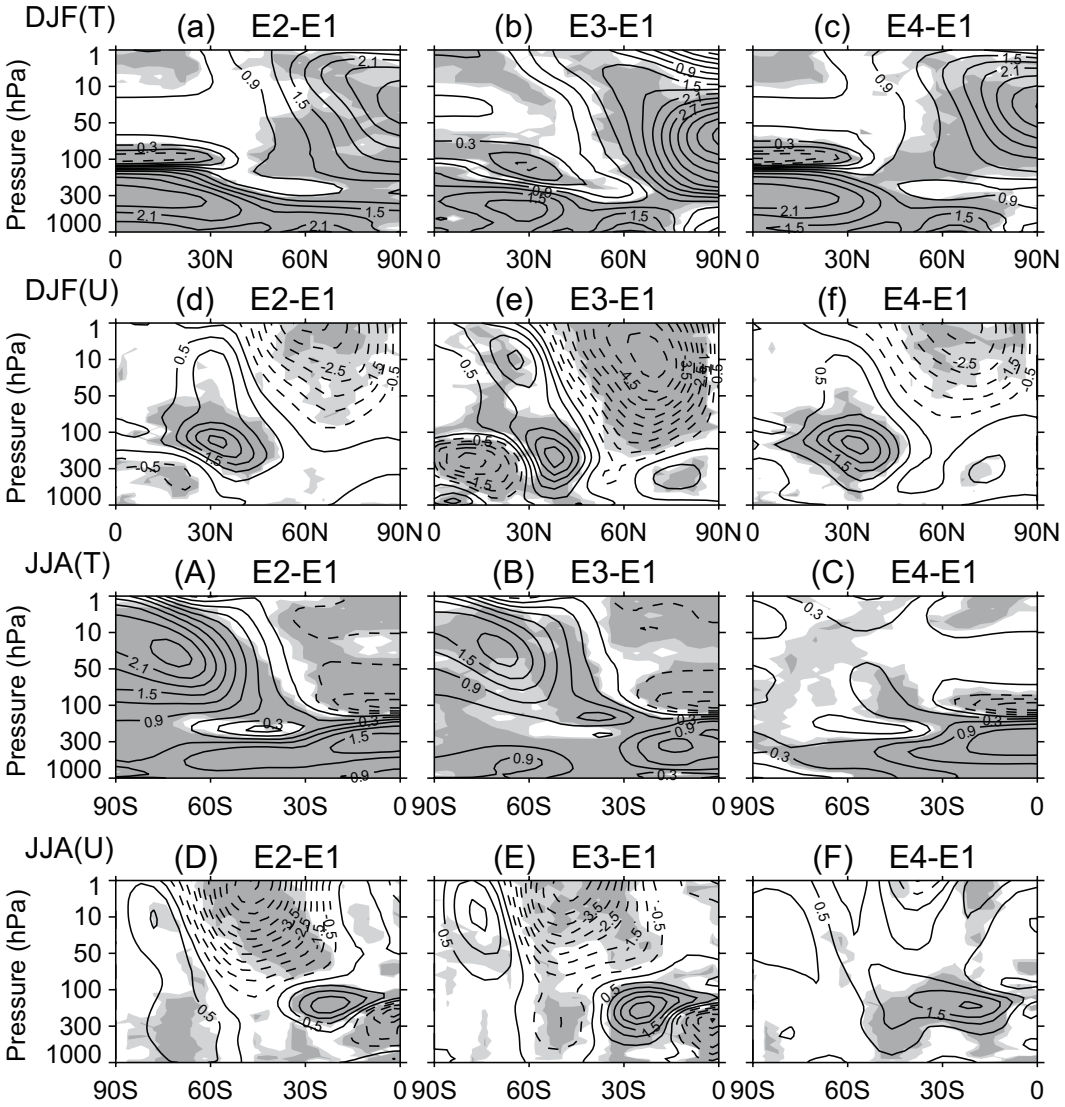

Fig. 6. DJF mean (a–c) temperature and (d–f) zonal wind differences in the NH between runs (a, d) E2 and E1, (b, e) E3 and E1 and (c, f) E4 and E1. JJA mean (A–C) temperature and (D–F) zonal wind differences in the SH between runs (A, D) E2 and E1, (B, E) E3 and E1 and (C, F) E4 and E1. The contour intervals for temperature and zonal wind differences are 0.3 K and 0.5 m s^{-1}, respectively. The regions where differences are statistically significant at the 95% (99%) level are shaded light (dark) grey. Solid and dashed lines represent positive and negative contours, respectively.

the southern polar vortex, but significant weakening of westerlies could be noted in the mid-latitude upper troposphere in runs E2 and E3.

The asymmetric responses of the northern and southern stratosphere to SST meridional gradient changes and different stratospheric temperature and zonal wind responses among the three runs may also have been related to different wave properties and wave propagation. Limpasuvan and Hartmann (2000) pointed out that high frequency transient waves contribute to the majority of total eddy forcing in the SH, while stationary waves control the eddy momentum fluxes in the NH. It is known that stationary waves are due to asymmetries at the Earth's surface, i.e., mountains, contrasting land–sea distributions, and SST asymmetries (e.g., Huang and Gambo, 1982). Therefore, it can be expected that SST increases of any type, as depicted in Fig. 1, will cause changes in the strength of stationary waves in the NH due to changes in land–sea surface temperature contrasts. Therefore, it is likely that the NH polar vortex is more sensitive to SST increases than the SH polar vortex, as can also be supported by Fig. 2, which shows that the northern polar stratosphere was warmed in all the three runs. In the SH, where the land–sea contrast is not dominant, the wave strength is expected to be more sensitive to magnitudes of SST changes. Note that the magnitude of SST increases was the largest in E2 and smallest in E4; therefore, the temperature response in the southern polar stratosphere was the largest and most significant in E2 (see Fig. 2). To provide more information on the effects of different SST changes on wave activities, Fig. 7 shows the differences in eddy heat flux ($\overline{v'T'}$) between different runs. The eddy heat flux is proportional to the vertical flux of wave activity via the EP flux (Dunkerton et al., 1981, Weber et al., 2003). Figure 7 indicates enhancements in planetary wave activities in the high-latitude troposphere in E2, E3 and E4. A slight enhancement of wave flux in the tropical and subtropical troposphere was also evident. The result here is consistent with Shepherd and McLandress (2011), who showed that the strengthening of the upper flanks of the subtropical jets allows more waves to penetrate into the subtropical LS. The eddy heat flux changes in the NH caused by the SST increases were overall larger than in the SH. As mentioned earlier, the wave strength is expected to be more sensitive to magnitudes of SST changes in the SH. Figure 7 indeed shows that a global uniform 1.0 K SST increase caused the largest eddy heat flux changes in the SH, while the gradient SST increases between 60°N–60°S caused relatively smaller eddy heat flux changes.

On the other hand, the wave propagation in both the NH and the SH is sensitive to zonal wind structure in the vertical direction, which is largely affected by SST meridional gradients via the thermal wind balance relationship. Chen and Robinson (1992) showed that a smaller vertical gradient of buoyancy frequency, N^2, and smaller zonal wind shear, tend to enhance the probability of wave propagation. Li et al. (2007) also argued that a larger vertical gradient of N^2 tends to reduce the probability of wave propagation. To further understand the effects of SST increases on the propagation

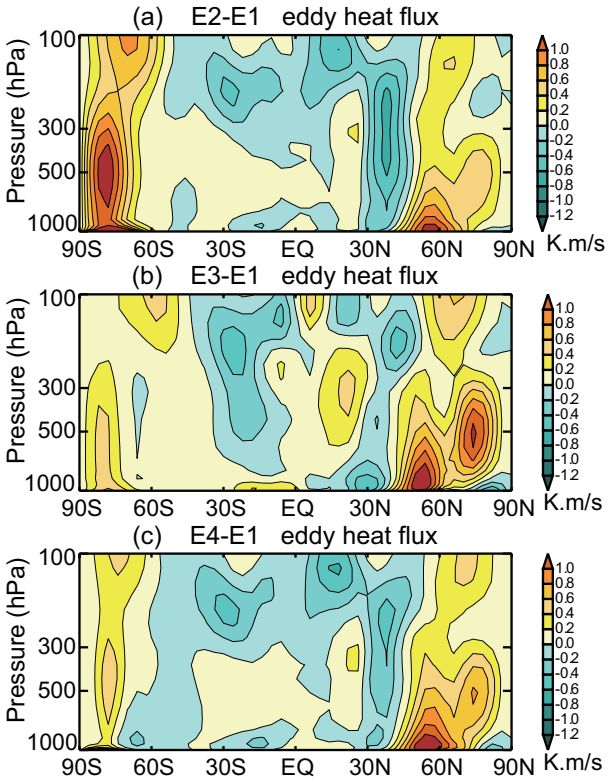

Fig. 7. The differences in annual mean eddy heat flux ($\overline{v'T'}$) between runs (a) E2 and E1, (b) E3 and E1, and (c) E4 and E1.

of waves, Fig. 8 shows the changes in vertical gradient of N^2 and the changes in zonal wind shear caused by different SST increases. SST increases seemed to have an evident impact on the vertical gradient of N^2 in the UTLS region. At the lower latitudes between 30°N–30°S, the SST increases in runs E2, E3 and E4 caused a decrease in the vertical gradient of N^2 below the tropopause level and an increase above the tropopause level. At mid-latitudes, the effect of the SST increases on the vertical gradient of N^2 was opposite to that at lower latitudes, i.e., the SST increases caused a decrease in the vertical gradient of N^2 above the tropopause level and an increase around the tropopause level. The changes in the vertical gradient N^2 in the UTLS region caused by a global uniform 1.0 K SST were largest in run E2. At mid-latitudes, the increases in the vertical gradient of N^2 in the UTLS region caused by the gradient increases of SST in runs E3 and E4 were smaller than in run E2; therefore, the planetary waves originating in the troposphere in runs E3 and E4 were more likely to propagate into the stratosphere and lead to a warming of the polar stratosphere.

As expected, the SST increases also caused changes in vertical zonal wind shear. Overall, the SST increases in runs E2–E4 caused an increase in zonal wind shear below the tropopause and a decrease above the tropopause at lower latitudes. The SST meridional gradient changes in E3 caused the largest decreases in zonal wind shear in the UTLS region at mid-high latitudes. The smaller zonal wind shear at mid-high latitudes and larger wave flux in E3 (Fig. 7b) al-

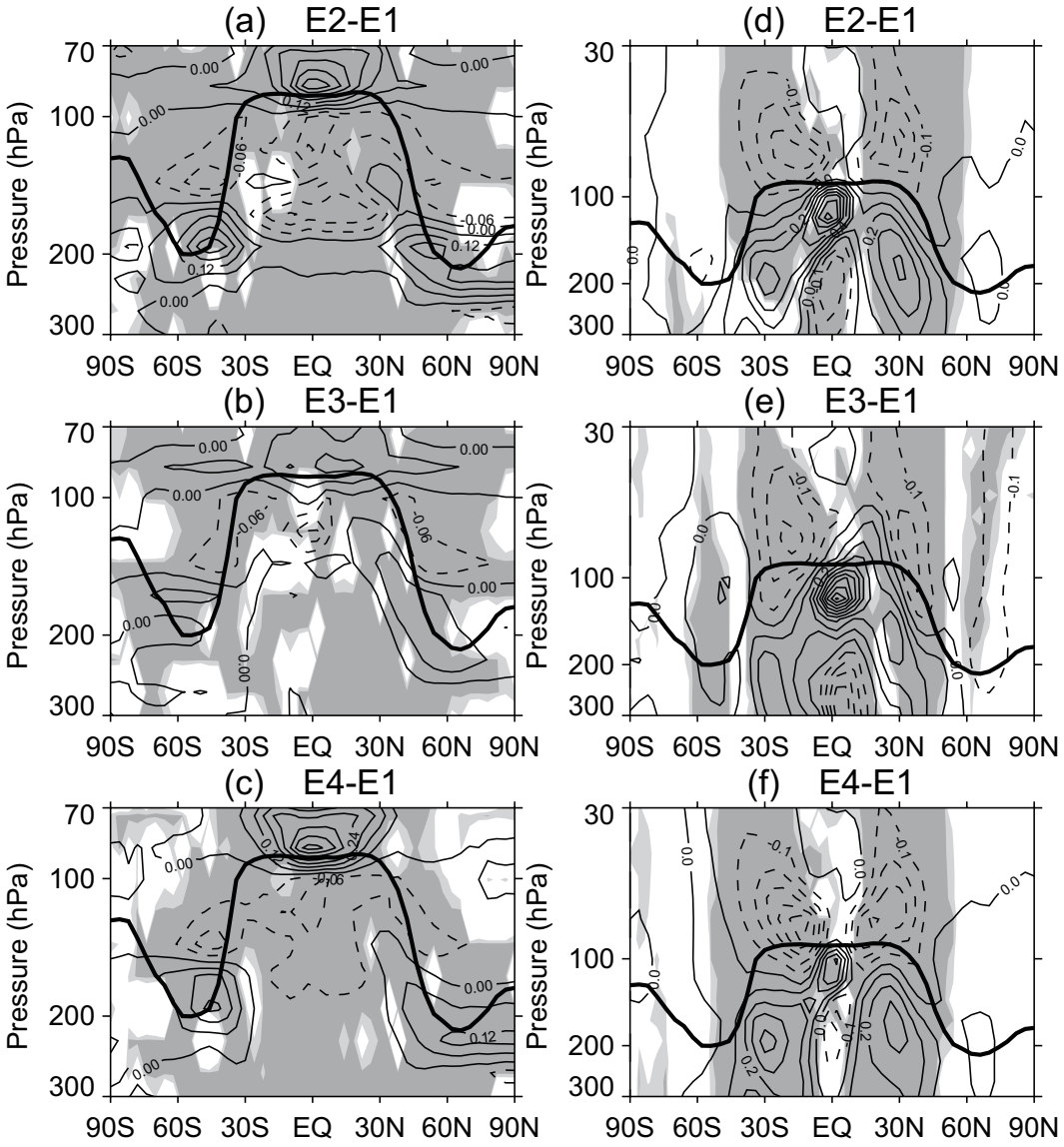

Fig. 8. (a–c) The differences in annual mean vertical gradient of buoyancy frequency (N^2) and (d–f) the differences in annual mean vertical zonal wind shear between runs (a, d) E2 and E1, (b, e) E3 and E1, and (c, f) E4 and E1. The contour intervals for the differences in the vertical gradient of N^2 and the differences in the vertical zonal wind shear are 0.06×10^{-7} m^{-1} s^{-2} and 0.1×10^{-3} s^{-1}, respectively. The thick black solid lines in the plots indicate the 40-yr mean cold-point tropopause height in the control run, E1. The regions where differences are statistically significant at the 95% (99%) level are shaded light (dark) grey. Solid and dashed lines represent positive and negative contours, respectively.

lowed more planetary waves to propagate upward into the polar stratosphere and cause the warmest Arctic polar stratosphere among the three runs. The zonal wind shear changes at high latitudes in runs E2 and E4 were rather small, while the eddy heat flux changes at mid-high latitudes in E2 were close to those in E4. Consequently, the temperature and zonal wind changes in the Arctic polar stratosphere in E2 and E4 were similar. These arguments can also be supported by the anomalous EP flux vectors shown in Figs. 4a–c, which indicate that the enhancement of upward wave propagation in the northern mid-high-latitude stratosphere was most pronounced in E3.

The above analysis indicates that the effect of SST increases on wave propagation is complex. Although SST increases may give rise to stronger waves, the vertical propagation of tropospheric waves into the stratosphere tends to be suppressed in the UTLS region at mid-latitudes due to an enhanced vertical gradient of N^2. SST increases have a significant effect on zonal wind shear both in the troposphere and stratosphere at lower latitudes, but this effect is not significant at high latitudes.

The radiative heating rate changes between different runs (not shown) indicates that the warming of the polar stratosphere in E2, E3 and E4 resulted mostly from the dynamic

effects of the SST increases, as the net radiative effect of the SST increases actually caused a cooling in the mid-high-latitude stratosphere.

4. Effects of SST changes on the BDC and tropopause

The results presented in section 3 showed that SST changes can affect stratospheric temperatures and circulation by altering forcing by waves. In this section, we focus on clarifying the effect of SST meridonal gradient changes on the BDC and the tropopause. Some earlier studies have shown convincing evidence that tropical warming can strengthen the BDC (e.g., Eichelberger and Hartmann, 2005) and that SST increases dominate the enhancement of BDC (e.g., Kodama et al., 2007). Here, we attempt to quantitatively diagnose the response of the BDC to SST gradient changes.

Table 1 lists the net upward and downward mass flux associated with the BDC at 72 hPa in terms of the mass stream function defined in Austin et al. (2003). Note that a global uniform 1.0 K SST increase (in E2) caused a 4.3% increase in the tropical upward mass flux at 72 hPa. The non-uniform global SST increases in E3 caused an even larger increase of upward mass flux of 5.5%, and the non-uniform SST increases between 60°S and 60°N in E4 gave rise to the largest increase of upward mass flux by 13.9%. As the global mean SST increase in E4 was the smallest, while the SST meridional gradient change was the largest, these results suggest that amplitude of the SST gradient has greater effects on tropical upwelling. These results can also be confirmed in terms of mid-high-latitude downwelling. For instance, the downwelling in the SH increased by 9.2% in E3 and 18.1% in E4, while the increase in E2 was the smallest (6.9%).

Some studies, such as Lamarque and Solomon (2010), suggested that ozone decreases in the tropical LS are mostly associated with acceleration in the tropical LS vertical velocity due to long-term increases in CO_2 and SSTs (e.g., Randel et al., 2006; Bekki et al., 2013). The ozone decreases in the LS in Fig. 3 indeed suggest a strengthened BDC, which would transport more ozone-poor air from the UT into the LS. Also note that the ozone decreases in the tropical LS were accompanied by ozone increases in the tropical mid-stratosphere (Fig. 3), suggesting a strengthening of the upward branch of the BDC there.

As the mean age-of-air is a good measure of bulk transport speed in the stratosphere associated with various transport processes (e.g., Hall and Plumb, 1994; Waugh and Hall, 2002), Fig. 9 was produced to show the changes in mean age-of-air caused by different SST changes. The SST increases in runs E2 to E4 all caused a decrease in the stratospheric mean age-of-air, implying that SST increases tend to accelerate upward transport in the stratosphere. This result is consistent with the results in previous studies (Deckert and Dameris, 2008; Shu et al., 2011). Overall, the mean age-of-air in the upper stratosphere was youngest in E4 and the oldest in E3 (Fig. 9a). This feature was particularly pronounced in the high-latitude stratosphere in both hemispheres. In the northern mid-latitude and southern high-latitude mid-stratosphere at 50 hPa, the mean age-of-air was youngest in E2 and oldest in E3 (Fig. 9b). The changes in mean age-of-air at 100 hPa caused by the SST increases became relatively small at lower latitudes, but were still large at high latitudes. Figure 9 indicates that responses of the transport speed to SST increases will be most pronounced in the high-latitude upper

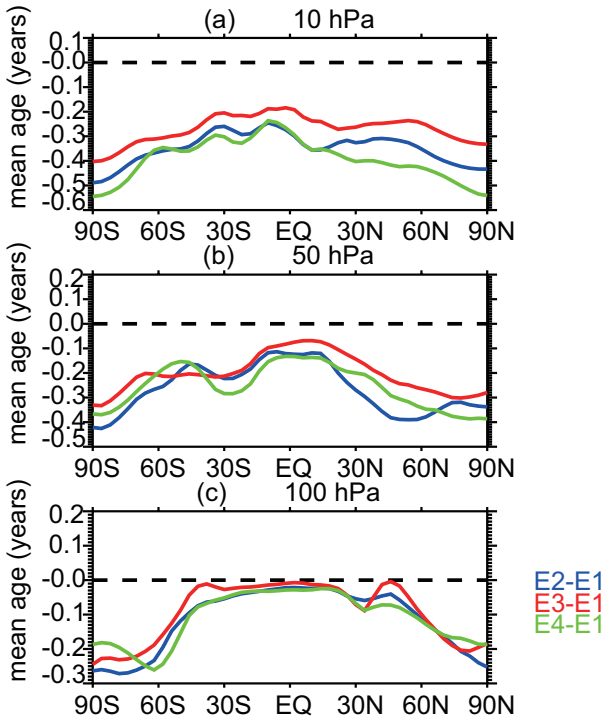

Fig. 9. The mean age-of-air differences between different runs (see the legend on the right-hand side of the figure) at (a) 10 hPa, (b) 50 hPa, and (c) 100 hPa.

Table 1. The mass flux (units: 10^9 kg s^{-1}) at 72 hPa in the different experiments. Positive and negative values denote upward and downward mass flux, respectively. Percentage changes of the mass flux (in parentheses) caused by SST changes in different experiments were estimated relative to that of the control run, E1.

Experiment	SH downwelling	Tropical upwelling	NH downwelling
E1	−3.48	+7.50	−4.09
E2	−3.72 (+6.9%)	+7.82 (+4.3%)	−4.17 (+2.0%)
E3	−3.80 (+9.2%)	+7.91 (+5.5%)	−4.13 (+1.0%)
E4	−4.11 (+18.1%)	+8.54 (+13.9%)	−4.47 (+9.3%)

stratosphere. It can also be inferred from the mean age-of-air differences between runs E3 and E4 that a larger SST gradient increase will tend to give rise to a younger mean age-of-air in the upper stratosphere. Note that the mean age-of-air changes are not only related to SST gradient changes, but also depend on the magnitude of SST changes. A global uniform 1.0 K SST increase with no gradient changes in E2 caused a younger mean age-of-air than in E3, in which the SST meridional gradient existed. The upward mass flux changes at 72 hPa listed in Table 1 were in accordance with the changes of mean age-of-air, i.e., a younger mean age-of-air corresponded with a larger upward mass flux. It should be pointed out that the changes in upward mass flux listed in Table 1 are only associated with the large-scale BDC and do not account for other transport processes. The mean age-of-air reflects an integrated transport property that is not only related to the large-scale BDC but also affected by various other transport processes, including meso- and synoptic-scale convective systems, small-scale mixing processes etc.

Figure 2 clearly shows that the SST increases caused a warming of the troposphere and a cooling in the tropical LS. It is necessary here to examine the tropopause height and temperature changes caused by the different changes of SST. Figure 10 shows the changes in the annual mean thermal tropopause [World Meteorological Organization definition (1957): the lowest level at which the average lapse rate is less than 2 K km^{-1} for 2 km ($-dT/dz < 2$)] and cold-point tropopause (the level where the temperature is the lowest between the troposphere and stratosphere) height and temperature between 30°S and 30°N relative to that in the control run, E1. It is apparent that SST increases in runs E2, E3 and E4 all resulted in a relatively higher tropical tropopause. The changes in both the thermal and cold-point tropopause height caused by the non-uniform SST increase between 60°S–60°N were the largest (E4), while the tropopause height changes caused by the SST meridional increases between the most northern and southern boundaries of the seas were the smallest (E3). Although SST increases tended to lift the tropical tropopause, the responses of the tropical tropopause temperature to different SST increases were not in phase with tropopause height changes, and the non-uniform SST increases with different gradients in E3 and E4 resulted in different tropical tropopause temperatures changes. The tropopause temperature changes in the tropics in E4 were relatively smaller than those in E2 and E3, although the tropopause height changes in E4 were larger than those in E2 and E3. Particularly noticeable was that the non-uniform SST increases in E3 tended to warm the subtropical

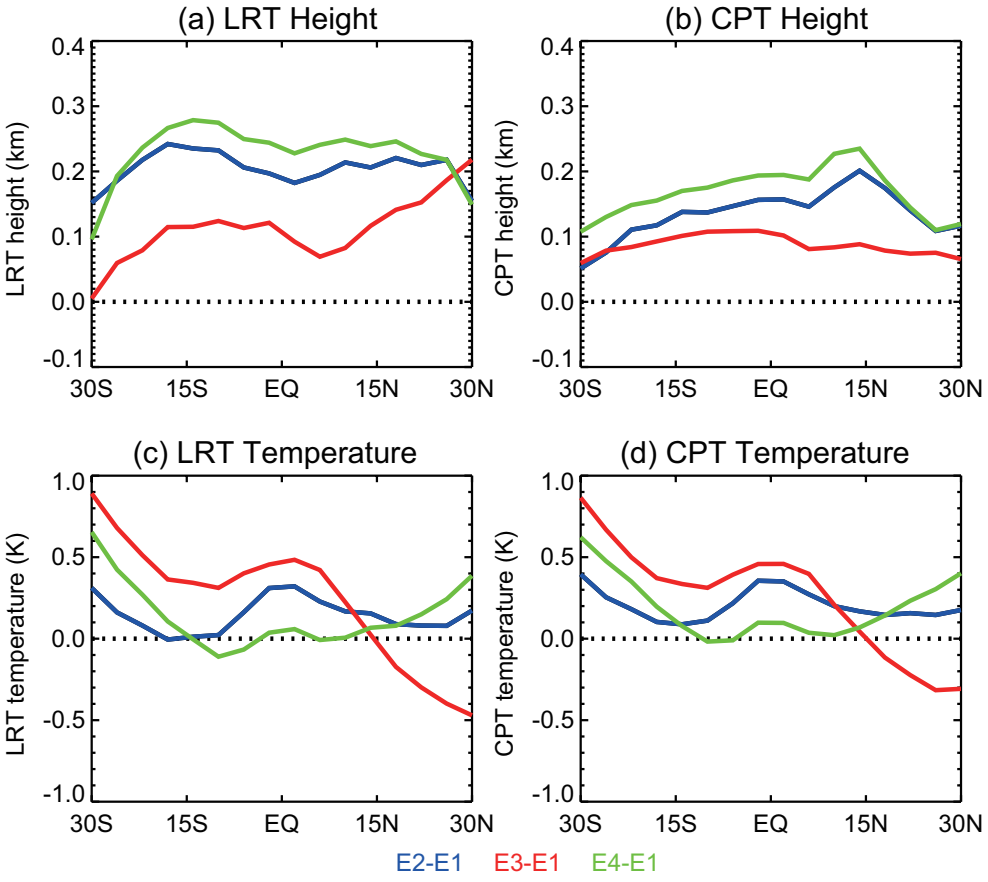

Fig. 10. Differences in annual and zonal mean thermal tropopause (a) height, (c) temperature and cold-point tropopause (b) height, (d) temperature within the 30°S–30°N latitude band. Different colored lines represent differences between different runs as depicted in the legend at the bottom of the figure.

tropopause in the SH but cool the subtropical tropopause in the NH. This latitudinal tropopause variation in E3 was in accordance with the temperature changes in Fig. 2b, which shows that the temperature increases in the southern extratropical UT were larger than those in the northern extratropical UT. The warming of the tropopause caused by the different SST increases was consistent with the warming of the UT (Fig. 2). Although lifting of the tropopause implies adiabatic cooling of the tropopause, the tropopause temperature changes would have resulted from the balance of the warming of the UT and the cooling of the LS (Santer et al., 2003). A lifted and warmer tropopause under higher SSTs suggests that warming of the troposphere due to SST increases dominates the tropopause temperature changes. This result is consistent with Gettelman et al. (2009), who showed that the tropopause is projected to be lifted and warmed in the future based on different CCM simulations.

5. Summary and conclusions

The results of the present reported set of model experiments suggest that SST increases accompanied by meridional gradient changes have a large impact on the stratosphere. In the model runs, both uniform and non-uniform SST increases tended to intensify the subtropical westerly jets. However, SST meridional gradient changes had a larger impact on zonal circulations than global uniform SST changes, particularly in the UTLS at mid and lower latitudes. SST gradient increases produced a larger and more significant impact on the northern polar stratosphere than on the southern polar stratosphere, and SST increases tended to weaken the northern polar vortex.

The asymmetric responses of the northern and southern polar stratosphere to SST meridional gradient changes were found to be mainly related to different wave transmissions and wave strengths in the NH and SH. SST increases tended to enhance the upward wave propagation in the mid-latitude lower troposphere, and this effect was more pronounced at northern mid-high latitudes. The results also suggested that SST increases can cause changes in the vertical gradient of buoyancy frequency in the UTLS region, as well as changes in vertical zonal wind shear, and that these changes can affect the upward wave propagation from the troposphere into the stratosphere. We noticed that the changes in the vertical gradient of buoyancy frequency at lower latitudes caused by SST increases had reversed signs above and below the tropopause, and this pattern was reversed in the mid-latitude UTLS. Both uniform and non-uniform SST increases resulted in an increase in the zonal wind shear below the tropopause and a decrease above the tropopause at lower latitudes. The effect of SST increases on zonal wind shear was not significant at high latitudes.

Finally, both the magnitudes of SST changes and SST meridional gradient changes were found to be important in modifying the large-scale BDC, with the latter having the greater impact of the two. Compared with global uniform SST increases, our results suggested that non-uniform SST increases with meridional gradient changes can cause larger changes in the mean age-of-air in the stratosphere and a larger increase in tropical upwelling.

Acknowledgements. This work was supported by the National Basic Research Program of China (Grant No. 2010CB428604) and the National Natural Science Foundation of China (Grant Nos. 41175042 and 41225018). We also thank the Fundamental Research Funds for the Central Universities of China (Grant No. lzujbky-2012-k04). We thank Prof. M. CHIPPERFIELD for help with the manuscript and helpful comments from the two anonymous reviewers.

REFERENCES

Austin, J., and Coauthors, 2003: Uncertainties and assessments of chemistry-climate models of the Stratosphere. *Atmospheric Chemistry and Physics*, **3**, 1–27.

Bekki, S., and Coauthors, 2013: Climate impact of stratospheric ozone recovery. *Geophys. Res. Lett.*, **40**(11), 2796–2800, doi: 10.1002/grl.50358.

Brierley, C. M., and A. V. Fedorov, 2010: Relative importance of meridional and zonal sea surface temperature gradients for the onset of the ice ages and Pliocene-Pleistocene climate evolution. *Paleoceanography*, **25**, PA2214, doi: 10.1029/2009PA001809.

Butchart, N., and Coauthors, 2006: Simulations of anthropogenic change in the strength of the Brewer-Dobson circulation. *Climate Dyn.*, **27**, 727–741.

Butchart, N., and Coauthors, 2010: Chemistry-climate model simulations of twenty-first century stratospheric climate and circulation changes. *J. Climate*, **23**, 5349–5374.

Calvo, N., R. R. Garcia, W. J. Randel, and D. R. Marsh, 2010: Dynamical mechanism for the increase in tropical upwelling in the lowermost tropical stratosphere during warm ENSO events. *J. Atmos. Sci.*, **67**, 2331–2340.

Chen, P., and W. A. Robinson, 1992: Propagation of planetary waves between the troposphere and stratosphere. *J. Atmos. Sci.*, **49**(24), 2533–2545.

Chen, W., and R. H. Huang, 2002: The propagation and transport effect of planetary waves in the Northern Hemisphere winter. *Adv. Atmos. Sci.*, **19**, 1113–1126.

Chen, W., H.-F. Graf, and M. Takahashi, 2002: Observed interannual oscillations of planetary wave forcing in the Northern Hemisphere winter. *Geophys. Res. Lett.*, **29**(22), 30-1–34-4, doi: 10.1029/2002GL016062.

Chiang, J. C. H., Y. Kushnir, and A. Giannini, 2002: Deconstructing Atlantic intertropical convergence zone variability: influence of the local cross-equatorial sea surface temperature gradient and remote forcing from the eastern equatorial Pacific. *J. Geophys. Res.*, 107, ACL 3-1–ACL 3-19, doi: 10.1029/2000JD000307.

Deckert, R., and M. Dameris, 2008: Higher tropical SSTs strengthen the tropical upwelling via deep convection. *Geophys. Res. Lett.*, **35**, L10813, doi: 10.1029/2008GL033719.

Dunkerton, T., C.-P. F. Hsu, and M. E. McIntyre, 1981: Some Eulerian and Lagrangian diagnostics for a model stratospheric warming. *J. Atmos. Sci.*, **38**, 819–843.

Eichelberger, S. J., and D. L. Hartmann, 2005: Changes in

the strength of the Brewer-Dobson circulation in a simple AGCM. *Geophys. Res. Lett.*, **32**, L15807, doi: 10.1029/2005GL022924.

Eyring, V., and Coauthors, 2005: A strategy for process-oriented validation of coupled chemistry-climate models. *Bull. Amer. Meteor. Soc.*, **86**, 1117–1133.

Eyring, V., and Coauthors, 2006: Assessment of temperature, trace species, and ozone in chemistry-climate model simulations of the recent past. *J. Geophys. Res.*, **111**, D22308, doi: 10.1029/2006JD007327.

Feng, J., J. P. Li, and F. Xie, 2013: Long-term variation of the principal mode of boreal spring Hadley circulation linked to SST over the Indo-Pacific warm pool. *J. Climate*, **26**, doi: 10.1175/JCLI-D-12-00066.1.

Garcia, R. R., and W. J. Randel, 2008: Acceleration of the Brewer-Dobson circulation due to increases in greenhouse gases. *J. Atmos. Sci.*, **65**, 2731–2739.

Garcia, R. R., D. R. Marsh, D. E. Kinnison, B. A. Boville, and F. Sassi, 2007: Simulation of secular trends in the middle atmosphere, 1950-2003. *J. Geophys. Res.*, **112**, D09301, doi: 10.1029/02006JD007485.

Gettelman, A., and Coauthors, 2009: The tropical tropopause layer 1960–2100. *Atmospheric Chemistry and Physics*, **9**, 1621–1637.

Hall, T. M., and R. A. Plumb, 1994: Age as a diagnostic of stratospheric transport. *J. Geophys. Res.*, **99**, 1059–1070.

Hoerling, M. P., J. W. Hurrell, and T. Xu, 2001: Tropical origins for recent North Atlantic climate change. *Science*, **292**, 90–92.

Huang, R. H., and K. Gambo, 1983: The response of a hemispheric multi-level model atmosphere to forcing by topography and stationary heat sources in summer. *J. Meteor. Soc. Japan*, **61**, 495–509.

IPCC, 2007: *Climate Change 2007: The Physical Science Basis*. *Contribution of Working Group I to the Fourth Assessment Report of the Intergovernmental Panel on Climate Change*, S. Solomon et al., Eds., Cambridge University Press, New York, 996 pp.

Kodama, C., T. Iwasaki, K. Shibata, and S. Yukimoto, 2007: Changes in the stratospheric mean meridional circulation due to increased CO_2: Radiation- and sea surface temperature-induced effects. *J. Geophys. Res.*, **112**, D16103, doi: 10.1029/2006JD008219.

Lamarque, J. F., and S. Solomon, 2010: Impact of changes in climate and halocarbons on recent lower stratosphere ozone and temperature trends. *J. Climate*, **23**, 2599–3611, doi: 10.1175/2010JCLI3179.1.

Li, Q., H. F. Graf, and M. A. Giorgetta, 2007: Stationary planetary wave propagation in Northern Hemisphere winter-climatological analysis of the refractive index. *Atmospheric Chemistry and Physics*, **7**, 183–200.

Limpasuvan, V., and D. L. Hartmann, 2000: Wave-maintained annular modes of climate variability. *J. Climate*, **13**, 4414–4429.

Magnusdottir, G., C. Deser, and R. Saravanan, 2004: The effects of North Atlantic SST and sea ice anomalies on the winter circulation in CCM3. Part I: Main features and storm track characteristics of the Response. *J. Climate*, **17**, 5857–5876.

Manzini, E., M. A. Giorgetta, M. Esch, L. Kornblueh, and E. Roeckner, 2006: The influence of sea surface temperatures on the Northern winter stratosphere: ensemble simulations with the MAECHAM5 model. *J. Climate*, **19**, 3863–3881.

Olsen, M. A., M. R. Schoeberl, and J. E. Nielsen, 2007: Response of stratospheric circulation and stratosphere-troposphere exchange to changing sea surface temperatures. *J. Geophys. Res.*, **112**, D16104, doi: 10.1029/2006JD008012.

Randel, W. J., F. Wu, H. Vöemel, G. E. Nedoluha, and P. Forster, 2006: Decreases in stratospheric water vapor after 2001: links to changes in the tropical tropopause and the Brewer-Dobson circulation. *J. Geophys. Res.*, **111**, 312, doi: 10.1029/2005JD006744.

Rind, D., R. Suozzo, N. K. Balachandran, and M. J. Prather, 1990: Climate change and the middle atmosphere. Part I: The doubled CO_2 climate. *J. Atmos. Sci.*, **47**, 475–494.

Santer, B. D., and Coauthors, 2003: Contributions of anthropogenic and natural forcing to recent tropopause height changes. *Science*, **301**, 479–483, doi: 10.1126/science.1084123.

Sassi, F., D. Kinnison, B. A. Boville, R. R. Garcia, and R. Roble, 2004: Effect of El Niño-Southern Oscillation on the dynamical, thermal, and chemical structure of the middle atmosphere. *J. Geophys. Res.*, **109**, D17108, doi: 10.1029/2003JD004434.

Seager, R., N. Harnik, Y. Kushnir, W. Robinson, and J. Miller, 2003: Mechanisms of hemispherically symmetric climate variability. *J. Climate*, **16**, 2960–2978.

Shepherd, T. G., and C. McLandress, 2011: A robust mechanism for strengthening of the Brewer-Dobson circulation in response to climate change: Critical-Layer control of subtropical wave breaking. *J. Atmos. Sci.*, **68**, 784–797.

Shu, J. C., W. Tian, J. Austin, M. P. Chipperfield, F. Xie, and W. K. Wang, 2011: Effects of sea surface temperature and greenhouse gas changes on the transport between the stratosphere and troposphere. *J. Geophys. Res.*, **116**, doi: 10.1029/2010JD014520.

Solomon, S., and Coauthors, 2007: *Climate Change 2007*: *The Physical Science Basis: Working Group I Contribution to the Fourth Assessment Report of the IPCC* Cambridge University Press, Cambridge, 1008 pp.

Waugh, D. W., and T. M. Hall, 2002: Age of stratospheric air: Theory, observations, and models. *Rev. Geophys.*, **40**(4), 1010, doi: 10.1029/2000RG000101.

Weber, M., S. Dhomse, F. Wittrock, A. Richter, B. Sinnhuber, and J. P. Burrows, 2003: Dynamical control of NH and SH winter/spring total ozone from GOME observations in 1995-2002. *Geophys. Res. Lett.*, **30**, 1583, doi: 10.1029/2002GL016799.

World Meteorological Organization, 1957: Meteorology—A three-dimensional science: Second session of the commission for aerology, *WMO Bull*, **4**, 134–138.

Xie, F., W. S. Tian, and M. P. Chipperfield, 2008: Radiative effect of ozone change on stratosphere-troposphere exchange. *J. Geophys. Res.*, **113**, D00B09, doi: 10.1029/2008JD009829.

Xie, F., W. Tian, J. Austin, J. Li, H. Tian, J. Shu, and C. Chen, 2011: The effect of ENSO activity on lower stratospheric water vapor. *Atmospheric Chemistry and Physics Discussions*, **11**, 4141–4166.

Xie, F., J. Li, W. Tian, J. Feng, and Y. Huo, 2012: Signals of El Niño Modoki in the tropical tropopause layer and stratosphere. *Atmospheric Chemistry and Physics Discussions*, **12**, 5259–5273.